



Measurement uncertainties in PSICAM and reflective tube absorption meters

INA LEFERING,^{1,*} RÜDIGER RÖTTGERS,² CHRISTIAN UTSCHIG,² MICHAEL S. TWARDOWSKI,³ AND DAVID MCKEE

¹Physics Department, University of Strathclyde, Glasgow, Scotland, UK

²Remote Sensing Department, Helmholtz-Zentrum Geesthacht, Geesthacht, Germany

³Harbor Branch Oceanographic Institute, Florida Atlantic University, Fort Pierce, FL, USA

*katharina.lefering@strath.ac.uk

Abstract: The nature and magnitude of measurement uncertainties (precision and accuracy) associated with two approaches for measuring absorption by turbid waters (b(532 nm) ranging from 0.20 m⁻¹ to 22.89 m⁻¹) are investigated here: (a) point source integrating cavity absorption meters (PSICAM), and (b) reflective tube absorption meters (AC-9 and AC-s – both WET Labs Inc., USA). Absolute measurement precision at 440 nm was quantified using standard deviations of triplicate measurements for the PSICAM and de-trended, bin averaged time series for the AC-9/s, giving comparable levels (< 0.006 m⁻¹) for both instruments. Using data collected from a wide range of UK coastal waters, PSICAM accuracy was assessed by comparing both total non-water absorption and absorption by coloured dissolved organic material (CDOM) measured on discrete samples by two independent PSICAMs. AC-9/s performance was tested by comparing total non-water absorption measured *in situ* by an AC-9 and an AC-s mounted on the same frame. Results showed that the PSICAM outperforms AC-9/s instruments with regards to accuracy, with average spread in the PSICAM total absorption data of 0.006 m⁻¹ (RMSE) compared to 0.028 m⁻¹ for the AC-9/s devices. Despite application of a state of the art scattering correction method, the AC-9/s instruments still tend to overestimate absorption compared to PSICAM data by on average 0.014 m⁻¹ RMSE (AC-s) and 0.043 m⁻¹ RMSE (AC-9). This remaining discrepancy can be largely attributed to residual limitations in the correction of AC-9/s data for scattering effects and limitations in the quality of AC-9/s calibration measurements.

Published by The Optical Society under the terms of the [Creative Commons Attribution 4.0 License](#). Further distribution of this work must maintain attribution to the author(s) and the published article's title, journal citation, and DOI.

OCIS codes: (010.1030) Absorption; (010.4450) Oceanic optics.

References and links

1. M. R. Lewis, M. E. Carr, G. C. Feldman, W. Esaias, and C. McClain, "Influence of penetrating solar-radiation on the heat budget of the equatorial pacific-ocean," *Nature* **347**(6293), 543–545 (1990).
2. A. Morel and L. Prieur, "Analysis of variation in ocean color," *Limnol. Oceanogr.* **22**(4), 709–722 (1977).
3. S. Sathyendranath and T. Platt, "Computation of aquatic primary production - extended formalism to include effect of angular and spectral distribution of light," *Limnol. Oceanogr.* **34**(1), 188–198 (1989).
4. A. Morel, "Optical Modeling of the upper ocean in relation to its biogenous matter content (Case-I waters)," *J. Geophys. Res. Oceans* **93**(C9), 10749–10768 (1988).
5. L. Prieur and S. Sathyendranath, "An optical classification of coastal and oceanic waters based on the specific spectral absorption curves of phytoplankton pigments, dissolved organic-matter and other particulate materials," *Limnol. Oceanogr.* **26**(4), 671–689 (1981).
6. H. R. Gordon, "Diffuse reflectance of the ocean: influence of nonuniform phytoplankton pigment profile," *Appl. Opt.* **31**(12), 2116–2129 (1992).
7. J. R. V. Zaneveld, R. Bartz, and J. C. Kitchen, "A reflective-tube absorption meter," *Proc. SPIE* **1302**, 124–136 (1990).
8. M. Twardowski, S. Freeman, S. Pegau, J. R. V. Zaneveld, J. Mueller, and E. Boss, "Chapter 2: Reflective tube absorption meters," in *NASA Ocean Optics Protocols, Vol I, Inherent Optical Property Measurements and Protocols*, A. Neely eds. In press (2018).

9. M. Twardowski, S. Freeman, S. Pegau, J. R. V. Zaneveld, J. Mueller, and E. Boss, "Chapter 1: The absorption coefficient, an overview," in *NASA Ocean Optics Protocols, Vol I, Inherent Optical Property Measurements and Protocols*, A. Neely eds. (2018).
10. G. Chang, A. Barnard, J. R. Zaneveld, and V. Zaneveld, "Optical closure in a complex coastal environment: particle effects," *Appl. Opt.* **46**(31), 7679–7692 (2007).
11. M. Tzortziou, J. R. Herman, C. L. Gallegos, P. J. Neale, A. Subramaniam, L. W. Harding, Jr., and Z. Ahmad, "Bio-optics of the Chesapeake Bay from measurements and radiative transfer closure," *Estuar. Coast. Shelf Sci.* **68**(1-2), 348–362 (2006).
12. C. Mitchell, A. Cunningham, and D. McKee, "Remote sensing of shelf sea optical properties: Evaluation of a quasi-analytical approach for the Irish Sea," *Remote Sens. Environ.* **143**, 142–153 (2014).
13. A. Tonizzo, M. Twardowski, S. McLean, K. Voss, M. Lewis, and C. Trees, "Closure and uncertainty assessment for ocean color reflectance using measured volume scattering functions and reflective tube absorption coefficients with novel correction for scattering," *Appl. Opt.* **56**(1), 130–146 (2017).
14. E. Boss, W. H. Slade, M. Behrenfeld, and G. Dall'Omo, "Acceptance angle effects on the beam attenuation in the ocean," *Opt. Express* **17**(3), 1535–1550 (2009).
15. R. V. Zaneveld, J. C. Kitchen, and C. Moore, "The scattering error correction of reflecting-tube absorption meters," *Proc. SPIE* **2258**, 44–55 (1994).
16. R. Röttgers, D. McKee, and S. B. Wozniak, "Evaluation of scatter corrections for ac-9 absorption measurements in coastal waters," *Methods Oceanogr.* **7**, 21–39 (2013).
17. N. D. Stockley, R. Röttgers, D. McKee, I. Lefering, J. M. Sullivan, and M. S. Twardowski, "Assessing uncertainties in scattering correction algorithms for reflective tube absorption measurements made with a WET Labs ac-9," *Opt. Express* **25**(24), A1139–A1153 (2017).
18. D. McKee, J. Piskozub, R. Röttgers, and R. A. Reynolds, "Evaluation and Improvement of an Iterative Scattering Correction Scheme for in situ Absorption and Attenuation Measurements," *J. Atmos. Ocean. Technol.* **30**(7), 1527–1541 (2013).
19. R. Röttgers, "Chapter 4: Point-Source Integrating-Cavity Absorption Meter (PSICAM)," in *NASA Ocean Optics Protocols, Vol I, Inherent Optical Property Measurements and Protocols*, A. Neely ed. (2018).
20. E. S. Fry, G. W. Kattawar, and R. M. Pope, "Integrating cavity absorption meter," *Appl. Opt.* **31**(12), 2055–2065 (1992).
21. R. M. Pope and E. S. Fry, "Absorption spectrum (380–700 nm) of pure water. II. Integrating cavity measurements," *Appl. Opt.* **36**(33), 8710–8723 (1997).
22. R. M. Pope, A. D. Weidemann, and E. S. Fry, "Integrating Cavity Absorption Meter measurements of dissolved substances and suspended particles in ocean water," *Dyn. Atmos. Oceans* **31**(1-4), 307–320 (2000).
23. L. Peperzak, H. J. van der Woerd, and K. R. Timmermans, "Disparities between in situ and optically derived carbon biomass and growth rates of the prymnesiophyte *Phaeocystis globosa*," *Biogeosci.* **12**(6), 1659–1670 (2015).
24. S. Pinet, J.-M. Martinez, S. Ouillon, B. Lartiges, and R. E. Villar, "Variability of apparent and inherent optical properties of sediment-laden waters in large river basins - lessons from in situ measurements and bio-optical modeling," *Opt. Express* **25**(8), A283–A310 (2017).
25. J. T. O. Kirk, "Point-source integrating-cavity absorption meter: theoretical principles and numerical modeling," *Appl. Opt.* **36**(24), 6123–6128 (1997).
26. R. A. Leathers, T. V. Downes, and C. O. Davis, "Analysis of a point-source integrating-cavity absorption meter," *Appl. Opt.* **39**(33), 6118–6127 (2000).
27. C. J. Y. Lerebourg, D. A. Pilgrim, G. D. Ludbrook, and R. Neal, "Development of a point source integrating cavity absorption meter," *J. Opt. A, Pure Appl. Opt.* **4**(4), S56–S65 (2002).
28. R. Röttgers, W. Schönfeld, P. R. Kipp, and R. Doerffer, "Practical test of a point-source integrating cavity absorption meter: the performance of different collector assemblies," *Appl. Opt.* **44**(26), 5549–5560 (2005).
29. R. Röttgers, C. Häse, and R. Doerffer, "Determination of the particulate absorption of microalgae using a point-source integrating-cavity absorption meter: verification with a photometric technique, improvements for pigment bleaching, and correction for chlorophyll fluorescence," *Limnol. Oceanogr. Methods* **5**(1), 1–12 (2007).
30. R. Röttgers, D. McKee, and C. Utschig, "Temperature and salinity correction coefficients for light absorption by water in the visible to infrared spectral region," *Opt. Express* **22**(21), 25093–25108 (2014).
31. I. Lefering, R. Röttgers, R. Weeks, D. Connor, C. Utschig, K. Heymann, and D. McKee, "Improved determination of particulate absorption from combined filter pad and PSICAM measurements," *Opt. Express* **24**(22), 24805–24823 (2016).
32. I. Lefering, F. Bengil, C. Trees, R. Röttgers, D. Bowers, A. Nimmo-Smith, J. Schwarz, and D. McKee, "Optical closure in marine waters from in situ inherent optical property measurements," *Opt. Express* **24**(13), 14036–14052 (2016).
33. R. Röttgers, D. Doxaran, and C. Dupouy, "Quantitative filter technique measurements of spectral light absorption by aquatic particles using a portable integrating cavity absorption meter (QFT-ICAM)," *Opt. Express* **24**(2), A1–A20 (2016).
34. I. Lefering, R. Röttgers, C. Utschig, and D. McKee, "Uncertainty budgets for liquid waveguide CDOM absorption measurements," *Appl. Opt.* **56**(22), 6357–6366 (2017).
35. R. Röttgers and R. Doerffer, "Measurements of optical absorption by chromophoric dissolved organic matter using a point-source integrating-cavity absorption meter," *Limnol. Oceanogr. Methods* **5**(5), 126–135 (2007).

36. J. M. Sullivan, M. S. Twardowski, J. R. V. Zaneveld, C. M. Moore, A. H. Barnard, P. L. Donaghay, and B. Rhoades, "Hyperspectral temperature and salt dependencies of absorption by water and heavy water in the 400-750 nm spectral range," *Appl. Opt.* **45**(21), 5294–5309 (2006).
37. M. S. Twardowski, J. M. Sullivan, P. L. Donaghay, and J. R. V. Zaneveld, "Microscale quantification of the absorption by dissolved and particulate material in coastal waters with an ac-9," *J. Atmos. Ocean. Technol.* **16**(6), 691–707 (1999).
38. C. Moore, J. R. V. Zaneveld, and J. C. Kitchen, "Preliminary results from an insitu spectral absorption meter," *Proc. SPIE* **1750**, 330–337 (1992).
39. R. V. Zaneveld, J. C. Kitchen, A. Bricaud, and C. Moore, "Analysis of insitu spectral absorption meter data," *Proc. SPIE* **1750**, 187–200 (1992).

1. Introduction

The absorption of visible light by marine waters plays a fundamental role in a variety of physical and bio-geochemical processes in the marine ecosystem. Absorption influences solar heating of the oceans [1], regulates the propagation of light underwater, contributes strongly to remote sensing reflectance [2], and affects primary production by affecting the amount and spectral distribution of light available for phytoplanktonic photosynthesis [3]. The spectral absorption coefficient is an inherent optical property (IOP), i.e., is independent from the light field and only determined by the medium (seawater) and constituents (dissolved and suspended) within. Absorption coefficient data are required to parameterise bio-optical models, including radiative transfer and primary production models, are used in the interpretation of ocean colour remote sensing signals, and can be used to estimate concentrations of non-water constituents [4–6].

Absorption spectra of dissolved (i.e. non-scattering) substances are routinely measured using simple spectrophotometric techniques. However, measuring absorption coefficients in a turbid (scattering) medium, such as seawater and in particular coastal waters, is more challenging because scattering by suspended material artificially increases the detected absorption signal, resulting in systematic overestimation of the true absorption coefficient. A range of absorption meter designs have been developed that attempt to resolve this issue.

The reflective tube absorption meter attempts to collect scattered light by using total internal reflection at the tube wall to redirect scattered photons towards a large area detector [7]. The WET Labs AC-9/s instrument series is based on this principle and has been widely used in the optical oceanography community for *in situ* measurements of spectral absorption, typically as depth profiles but also in flow-through systems, or on moored or towed platforms [8]. AC-9/s devices measure both spectral absorption and spectral attenuation coefficients simultaneously. Over the past two decades, these instruments have become the industry standard in the field (NASA protocols [8,9]) and have been widely used in studies investigating the propagation of light underwater [10,11] and in ocean color remote sensing validation activities [12,13]. However, both absorption and attenuation measurements suffer from significant scattering errors: the reflective tube absorption measurement fails to collect all scattered photons, while the attenuation measurement does not exclude all scattered light due to the relatively large collection angle (0.9 degrees in water [14]). To correct for these measurement artefacts, a number of AC-9/s scattering corrections have been developed over the years, correcting either just the absorption [15–17] or both absorption and attenuation measurements [18].

Another way to determine total absorption with high accuracy is with lab-based measurements of discrete, untreated water samples inside an integrating cavity [19,20]. As a result of multiple reflections at the cavity walls, these integrating cavity absorption meters (ICAMs) benefit from a long effective path length and high sensitivity. Scattering effects can be neglected if a homogeneous, diffuse light field is created inside the cavity. Some ICAM configurations use broadband, white light illumination and hyperspectral detectors, allowing for very short acquisition times at the expense of potential detector sensitivity issues, significant internal stray light and inelastic scattering artefacts. Pope and Fry [21] developed an ICAM and used it for the determination of pure water absorption coefficients and natural

water samples [22]. Commercial instruments based on the integrating cavity approach have recently become available (e.g., Trios OSCAR, the HOBI Labs a-Sphere (not available on the market) and the Turner Designs flow-through ICAM). All these instruments were designed as flow-through systems, but only a very small number of studies using these instruments has been published to date [23,24]. Kirk [25] proposed and theoretically described a point-source integrating-cavity meter (PSICAM), which uses an isotropic light source placed at the center of an integrating sphere. This set-up was later implemented and further investigated by Leathers et al. [26] and Lerebourg et al. [27]. Röttgers et al. [28] also developed a PSICAM set-up which has been used in a number of studies over the past decade [29,30]. PSICAM measurements have been shown to be effectively insensitive to the presence of scattering material [28]. The PSICAM probably represents the current state of the art for determination of absorption for natural water samples. Uptake of the technology by the optical oceanography community has been limited, however, largely because calibration and measurement protocols are labour intensive and require very careful sample handling. The potential value of investing time and effort into PSICAM measurements has recently been demonstrated through applications where PSICAM data was used to establish the performance of various AC-9/s scattering corrections [17,18] and to establish new methods to correct filter pad absorption data for path length amplification and scattering offset errors [31].

Recent optical closure studies have shown broad agreement between measured radiometric parameters and radiative transfer simulations based on *in situ* measurements of absorption and backscattering coefficients may be possible with absolute errors <20% [11,13,32]. This has strengthened confidence in the estimation of *in situ* optical properties in terms of overall magnitude and spectral distribution. However, there is still very little quantitative analysis of the precision and accuracy of these absorption measurement techniques, information which is required for the development of robust ocean color retrieval algorithms and population of bio-optical models. This work will quantify measurement uncertainties in determinations of total absorption coefficients with both PSICAM and AC-9/s devices, including a description of the nature and magnitude of errors. Results presented will be used to discuss the consistency of both methods (within each and between each other), estimates for measurement precision and the effects of sensor calibration on final absorption spectra.

2. Methods

2.1 Sampling location

Absorption data were collected during a cruise on *R/V Heincke*, circumnavigating Great Britain, in spring 2015. Sampling sites covered a wide range of different water types from sediment-dominated estuaries (Bristol Chanel with an maximum $b(532\text{nm})$ of 22.89 m^{-1}) to relatively clear waters north of Scotland ($b(532\text{ nm}) = 0.20\text{ m}^{-1}$). Details on the data set and the optical properties of the waters samples can be found in several previous publications [17,33,34]. Water samples were collected using Niskin bottles, mainly at depths close to the surface (top 10 m) plus a few at greater depths, up to 85 m. On board, samples were divided into 4 subsamples for independent PSICAM absorption measurements of both total absorption and coloured dissolved organic matter (CDOM) absorption by teams from the Helmholtz-Zentrum Geesthacht (HZG) and the University of Strathclyde (Strath).

2.2 PSICAM measurements

Both PSICAM set-ups used for this work were built following the description by Röttgers et al. [28,29] and are not currently available as a single commercial product. The cavities used in this study were made from OP.DI.MA (ODM98, Gigahertz-Optik Germany), a highly diffuse reflective material (98% reflectivity according to manufacturer) with an inner radius of

4.5cm. In both cases, the light source consisted of a 10.0 mm diameter diffuse quartz-glass sphere connected to an electronically stabilized 150 W halogen lamp (CF1000, Illumination Technology Inc., USA) using fibre optics and was placed in the centre of the integrating cavity. The light inside the cavity was collected by another quartz-glass fiber bundle, which was positioned so that the light source is outside its field of view, and was guided to a photodiode array spectrometer, AvaSpec ULS2048XL (Avantes, Netherlands). The Strath PSICAM used a sensor for the VIS-to-NIR range (ULS2048XL-RS-SPU2) while the HZG PSICAM used the UV-to-VIS version (ULS2048XL-SP-UB). The cavity was pre-soaked by filling it with ultrapure water for at least 12 hours and lamp and detector were allowed to stabilize for at least 1 hour before first measurements were taken.

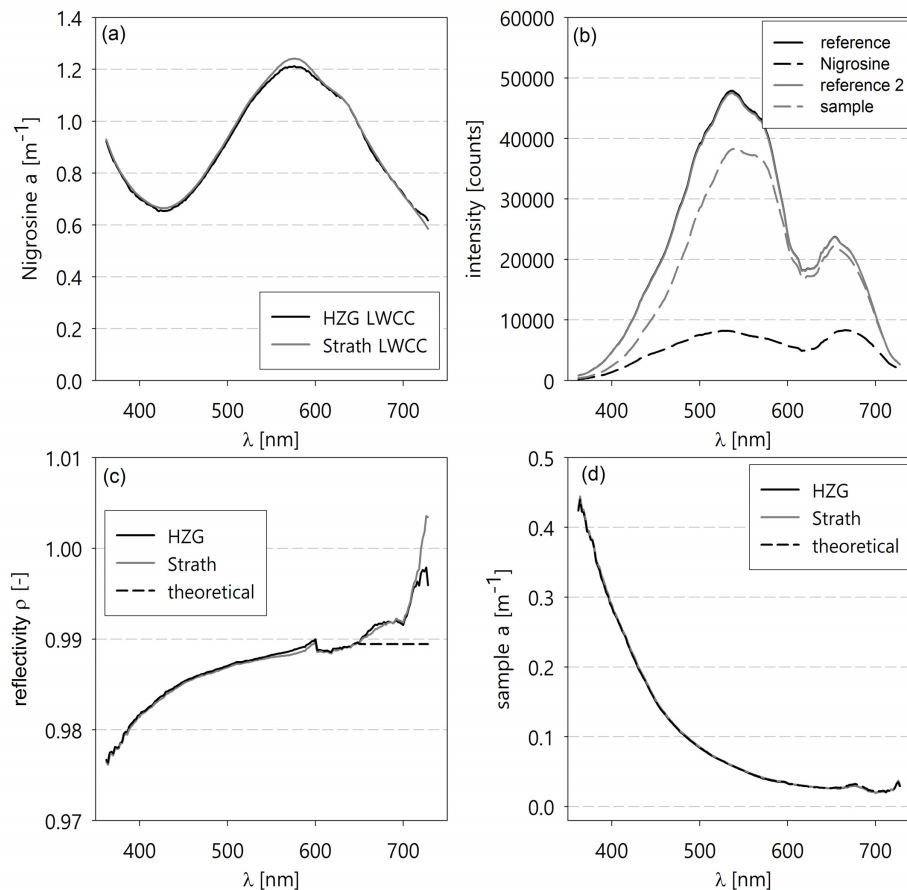


Fig. 1. Summary of measurements made for an example PSICAM calibration and subsequent sample absorption determination. (a) shows Nigrosine absorption spectra determined with two different LWCC systems; (b) shows light intensity spectra measured inside the PSICAM for transmission calculations (Nigrosine/reference for calibration and sample/reference 2 for sample absorption); (c) shows resulting PSICAM reflectivity spectra calculated using the data shown in (a) and (b); (d) shows the effect of different calibrations shown in (c) on PSICAM absorption data. The dashed line in (c) and (d) shows an idealized reflectivity spectrum and its impact on PSICAM absorption values.

The accuracy of PSICAM absorption measurements is limited by uncertainties in the calibration, i.e., the determination of the reflectivity of the inner cavity walls, ρ . Lerebourg et al. [27] have shown that a 1% error in the reflectivity can lead to a 10% error in the total sample absorption (i.e. including the absorption by water) measured in the PSICAM. The reflectivity is determined following the descriptions in Leathers et al. [26] and Röttgers and

Doerffer [35]. Two measurements are required to determine ρ : (1) a measurement of the PSICAM transmission of a calibration solution and (2) an independent measurement of the absorption of the calibration solution in a spectrophotometer.

The PSICAM was calibrated using a black dye called Nigrosine (Certistain, Merck, Germany) which absorbs broadly across the UV/VIS spectrum [Fig. 1(a)]. Every morning 5L of the calibration solution were prepared by filtering a few drops of concentrated Nigrosine stock solution through a pre-rinsed 13mm Spartan syringe filter (0.2 μm pore size; Whatman, UK) into ultrapure water. Both groups used fresh sub-samples of the Nigrosine solution for each calibration (3-5 times a day). Using the aliquots of the same calibration solution reduces potential artefacts and bias in PSICAM absorption data.

Prior to every calibration, the cavity was bleached with a weak sodium hypochlorite solution (about 1 mL of 6 - 14% NaOCl (Sigma Aldrich Co.) diluted in 1 L of purified water) for about 15 minutes and then rinsed thoroughly, first with tap water and finally with ultrapure water. The intensity inside the cavity was measured twice, first when filled with ultrapure water and secondly, when filled with the Nigrosine solution [Fig. 1(b)]. The cavity was bleached and rinsed every time it was filled with Nigrosine to eliminate the risk of contamination by the adhesive dye. After bleaching, a second measurement of the light intensity for a PSICAM filled with ultrapure water was made to check measurement stability. The transmission inside a PSICAM is determined by dividing the light intensity spectrum measured when the cavity is filled with the calibration solution (or sample) by the light intensity spectrum measured when the cavity is filled with the reference (ultrapure water; [Fig. 1(b)]). The temperature of each fluid inside the cavity was noted for temperature corrections during subsequent processing. Required corresponding measurements of Nigrosine absorption spectra were also made independently by the two groups, using two long path length systems (LWCC, World Precision Instruments Inc.; [Fig. 1(a)]). Both PSICAMs were calibrated daily, with at least three replicates being spread over the course of a day in order to monitor potential changes in the cavity's reflectivity. Variability between replicates was typically $< 1.5\%$.

The absorption by all non-water constituents of discrete, untreated samples was determined in both PSICAMs (HZG PSICAM and Strath PSICAM) in triplicate against ultrapure water as a reference between 362 – 728 nm. Absorption coefficients were calculated using the reflectivity as determined during calibration [Fig. 1(c)] and a measurement of transmission (sample intensity/reference intensity) in the PSICAM [Fig. 1(b)]. It should be noted that Fig. 1(c) shows apparently unphysical reflectance values (> 1) in the NIR – these are discussed later in the results section. Absorption spectra were corrected for temperature and salinity effects of pure water absorption using two sets (one for each set-up) of instrument-specific temperature and salinity correction factors [28,30] and for chlorophyll fluorescence effects [29,33]. The latter requires additional measurements of the light intensity inside the cavity when wavelengths of the fluorescence, i.e. at > 620 nm, are excluded from the illumination. Figure 1(d) shows a total absorption spectrum for a sample collected in the Irish Sea. Samples for CDOM measurements were filtered through a 0.22 μm pore size membrane filter (GSWP, Merck Millipore Ltd., Ireland), using a low vacuum < 0.2 bar and the absorption by CDOM was measured in triplicate, following the same protocol.

2.3 AC-9/s absorption measurements

In situ absorption spectra were measured with two reflective tube instruments, a multispectral AC-9 and a hyperspectral AC-s (both WET Labs Inc., USA). The AC-9 determines absorption at 9 different wavebands (FWHM = 10 nm), centred around 412 nm, 440 nm, 488 nm, 510 nm, 532 nm, 650 nm, 676 nm, and 715 nm, while the AC-s is configured to measure absorption hyperspectrally from 400 – 742 nm in ~ 4 nm intervals. Both instruments were equipped with 25-cm path length flow tubes equipped with quartz cuvettes and were mounted on the same frame together with a CTD (SBE19plus, SeaBird Scientific, USA) and an array

of Niskin bottles. AC-9/s absorption spectra were calculated as the median of a time series of several minutes (typically 2.5 – 5 min; with the shortest being just over 1 min and the longest just under 6 min), measured while the frame was kept stationary at a certain depth (to collect samples for PSICAM measurements). This ensured minimal bias due to temporal or spatial mismatch between PSICAM and AC-9/s absorption data. Concurrent CTD temperature and salinity data were used to correct AC-9/s absorption spectra for the effects of temperature and salinity [36].

Both AC-9/s devices were calibrated with ultrapure water (Milli-Q, Millipore) in the lab shortly before the cruise. Additional ultrapure water measurements were performed on board throughout the cruise to monitor potential drifts in the instruments [37]. In total twelve measurements of ultrapure water absorption were made with the AC-s on eight different days spread across the sampling period, whereas eight data sets (measured on seven days) were available for the AC-9. For each calibration, freshly prepared ultrapure water was pumped into the instrument while the stability of signals at all absorption and attenuation channels was monitored. Drifting signals were attributed to a variety of factors, including de-gassing, temperature changes or ship movement, in which case the cuvettes were flushed with more ultrapure water until a stable signal was observed. Once the signal was stable, the total non-water absorption was recorded for one minute and the median was calculated. CDOM absorption spectra were not measured with AC-9/s instruments and all further AC-9/s analysis and comparison is done on total non-water absorption data only.

Absorption measurements in AC-9/s instruments are based on a reflective tube approach to reduce scattering errors. Most scattered light is redirected to a diffuse detector using total internal reflection at the external air-quartz interface of the flow tube [38,39]. However, a significant portion of scattered light (particularly beyond the critical angle for total internal reflection [18]) does not reach the detector which can result in overestimation of absorption coefficients of > 80% [16]. Absorption data measured in AC-9/s devices therefore have to be corrected for scattering errors by applying one of several correction methods which have been proposed over the years. The most commonly used scattering correction is the proportional correction which assumes negligible absorption at a reference wavelength (typically 715 nm) and scales the absorption across the spectrum proportionally to the measured scattering signal relative to the scattering measured at the reference wavelength [15]. This approach was recently revised, replacing the assumption of negligible NIR absorption with an empirical relationship based on absorption spectra measured in a PSICAM (semi-empirical correction [16]).

$$a_{ac9}(\lambda) = a_m(\lambda) - [a_m(715) - a_{emp}(715)] \frac{(1/e_c)c_m(\lambda) - a_m(\lambda)}{(1/e_c)c_m(715) - a_{emp}(715)}, \quad (2)$$

where a_{ac9} is the corrected non-water absorption at a given wavelength, λ , a_m and c_m denote uncorrected measured absorption and attenuation signals. 715 nm is used as the reference NIR wavelength. $1/e_c$ is a scattering correction for the attenuation measurement [14] and $a_{emp}(715)$ is an empirical estimate of the NIR absorption coefficient and is given by:

$$a_{emp}(715) = 0.212 [a_m(715)]^{1.135}. \quad (3)$$

The semi-empirical correction is currently the most advanced correction method which does not require any additional optical data from other instruments. Since the aim here is to focus on the measurement uncertainties inherent to each absorption meter, all AC-9/s absorption data presented in this work has been corrected with the semi-empirical correction.

3. Results

3.1 PSICAM - variability in calibration

PSICAM calibrations made on the same day were averaged to determine daily reflectivity spectra which were used to assess the stability of the instruments and the robustness of the calibration procedure. Figure 2 shows little apparent variability in 18 daily reflectivity spectra determined for the HZG-PSICAM, generally less than 1% of the measured reflectivity across all wavelengths with the exception of two spectra that deviate up to 1.5% from the overall average at red/NIR wavelengths. Previous sensitivity analysis showed that a 1% error in the reflectivity can lead to an error of about 10% in the calculated PSICAM total sample absorption (i.e. including absorption by water itself) [27]. Figure 1 shows a practical demonstration of the sensitivity of PSICAM absorption measurements to uncertainties in reflectivity determination. Most notable is the lack of sensitivity to reflectivity errors in the red/NIR. The reflectivity is effectively a tuning variable used to match PSICAM data with absorption coefficients of the same Nigrosine solution measured with another spectrophotometer, modelling PSICAM performance. In practice, it can be greater than 1.0 at red/NIR wavelengths (even though this is theoretically ‘unphysical’) which can be attributed to increased measurement errors due to high water absorption, artefacts due to internal stray light issues of the detector, imperfect correction of temperature and salinity effects at these wavelengths, and the fact that the assumption of a totally homogeneous light field might not hold.

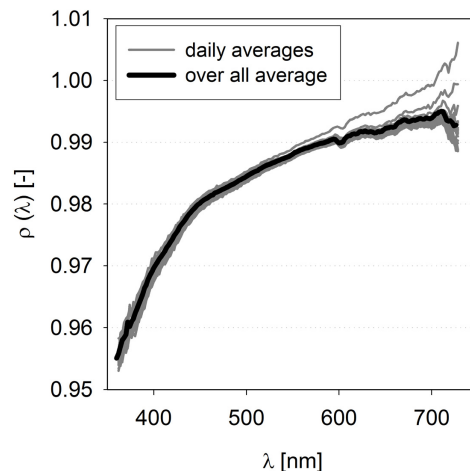


Fig. 2. Daily averages (grey lines, 18 daily averages) and overall average (black line) of reflectivity spectra obtained for calibration of the HZG PSICAM during a 20-day cruise from 362 to 728 nm.

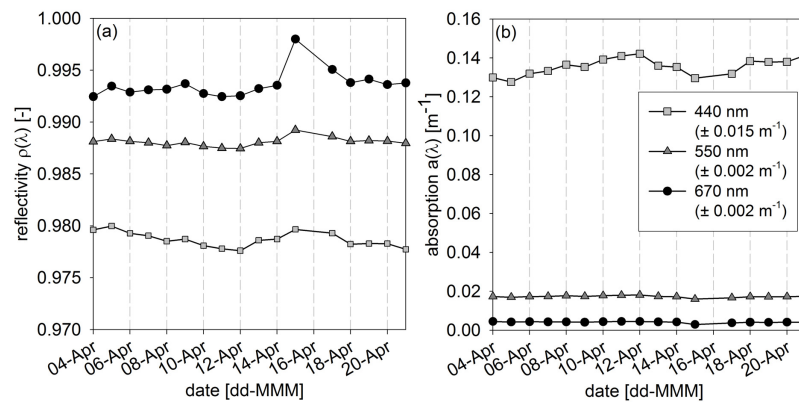


Fig. 3. (a) Time series of HZG PSICAM reflectivity (daily averages) at three different wavelengths, 440 nm, 550 nm, and 670 nm. (b) Sensitivity of PSICAM absorption coefficients to variability in the reflectivity. Plot shows the CDOM absorption of a single sample calculated using each of the daily reflectivity shown in (a) at three wavelengths, 440 nm, 550 nm, and 670 nm.

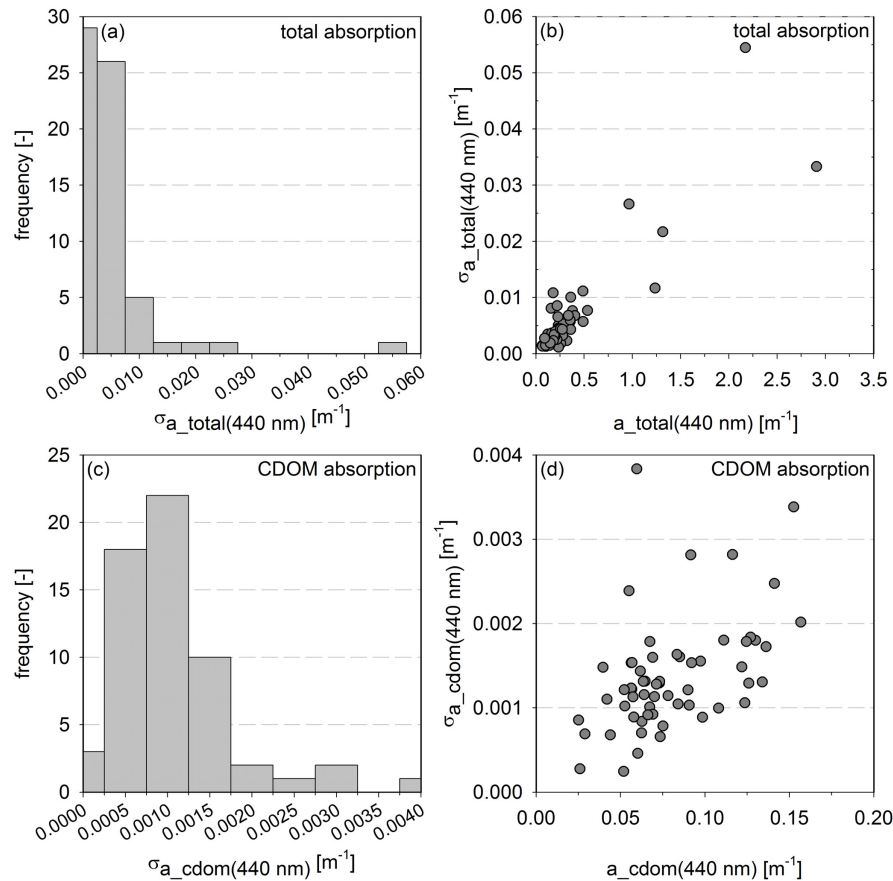


Fig. 4. Histogram of standard deviation derived from triplicates for Strath PSICAM (a) total non-water and (c) CDOM absorption measurements, both at 440 nm. Standard deviation vs. absorption at 440 nm for Strath PSICAM (b) total non-water and (d) CDOM absorption. Note the different scales for total non-water absorption and CDOM absorption standard deviations.

Figures 1(c) and 1(d) show an example where the assumption of a flat reflectivity at wavelengths > 600 nm changes the absorption by less than 0.0038 m^{-1} between $600 - 728$ nm, compared to absorption values derived from measured reflectivity. This very small absolute error is broadly consistent with Lerebourg et al. [27] as it constitutes a fractional error of 13.8% associated with an uncertainty of $\sim 1\%$ in the reflectivity. Of course, it is always important to consider whether the absolute or fractional error is more important, which is entirely dependent on how the data will be subsequently used.

If we assume that the observed variability in reflectivity is only due to measurement uncertainties, not due to real physical changes in reflectivity by e.g. optical contaminations, the effect on PSICAM absorption coefficients can be assessed using the full range of daily average values to calculate CDOM absorption coefficients for a single sample measurement at a blue, a green and a red wavelength [Fig. 3]. Results show that the sensitivity of absorption coefficients to variability in ρ is wavelength dependent. At the blue and green wavelength, the reflectivity varied by 0.0024 and 0.0017, causing variations in absorption of 0.0146 m^{-1} ($\pm 5.4\%$) and 0.0021 m^{-1} ($\pm 6.1\%$) respectively (% deviations relative to mean values). The largest variation of 0.0055 in the reflectivity was observed at 670 nm where it resulted in the smallest absolute change in absorption of 0.0015 m^{-1} , equivalent to $\pm 18.3\%$ compared to the average absorption coefficient of 0.0041 m^{-1} at this wavelength. The headline figure of 1% error in reflectivity causes 10% error in PSICAM absorption [27] can therefore not be taken as a definitive statistic for this source of error, but is a reasonable estimate of a typical error that in reality is both sample and wavelength dependent.

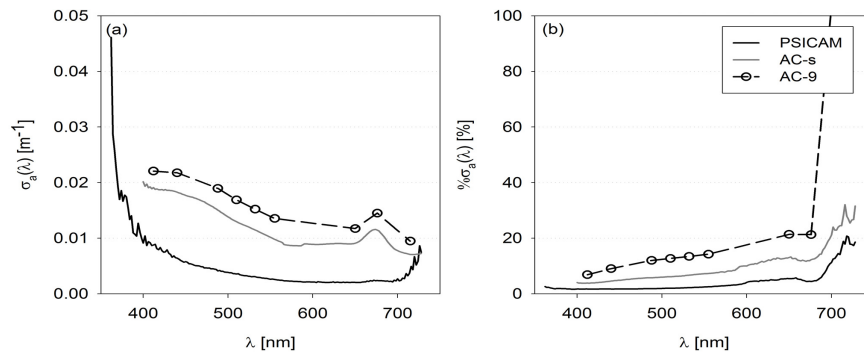


Fig. 5. Average spectral standard deviation of all total non-water absorption measurements, made with three different absorption meters (PSICAM, AC-9, AC-s) – (a) absolute and (b) relative compared to average absorption signal. AC-9/s standard deviations were derived from de-trended time series recorded when instruments were held at depth. PSICAM absorption measurements were performed on discrete samples collected at the same depths.

3.2 Precision of PSICAM measurements

Standard deviations of triplicate PSICAM measurements were used to assess measurement precision [Fig. 4]. A separate sub-sample was analysed for each of the triplicate measurements, so some of the observed variability can be attributed to inter-sample heterogeneity. Absorption coefficients at 440 nm ranged from 0.066 m^{-1} to 2.908 m^{-1} for total non-water absorption, and 0.025 m^{-1} to 0.157 m^{-1} for CDOM. Standard deviations at 440 nm determined for total non-water absorption [Fig. 4(a)] were generally $< \pm 0.01 \text{ m}^{-1}$ (87%) with 59% ($N = 63$) being within $\pm 0.004 \text{ m}^{-1}$. In general, standard deviations were found to increase with measured absorption signal at 440 nm [Fig. 4(b)] and largest standard deviations up to $\pm 0.055 \text{ m}^{-1}$ were observed for total samples collected in the Bristol Channel with generally high absorption of $> 0.9 \text{ m}^{-1}$ at 440 nm. Standard deviations for CDOM absorption measurements exhibited a similar trend [Fig. 4(c) and 4(d)] with standard

deviations $< \pm 0.004 \text{ m}^{-1}$ for all samples ($N = 59$). This reflects the fact that particle-free CDOM samples are more optically homogeneous than the original natural water samples.

The typical precision for total, non-water PSICAM absorption measurements of 0.006 m^{-1} (equivalent to 1.7%) was estimated by taking the average of all triplicate standard deviations. The resulting estimate of PSICAM precision was found to be wavelength dependent, in both absolute and relative terms, relatively flat from 500 to 700 nm but strongly increasing toward both edges of the spectrum, where light intensity levels drop toward the detection limit [Fig. 5].

3.3 PSICAM accuracy / data consistency

Assessment of accuracy generally requires some independent measure of truth against which an observation can be tested. Unfortunately, no such standard is easily available for these kinds of measurements, so comparison of data from two independently operated instruments is the best that can be achieved, being aware that there might be systematic biases inherent to the optics setup, such as uncorrected detector issues (e.g. non-linearity and internal stray light). Strictly speaking, this is only a test of consistency but it is as close to a measure of accuracy as is currently possible. Figure 6(a) shows total non-water absorption data from 362 – 728 nm measured with both PSICAMs plotted against each other. Overall, data followed a linear relationship with a geometric mean linear regression slope of 1.02 and an R^2 of 0.997 (Table 1). At wavelengths $> 650 \text{ nm}$, i.e. at low absorption coefficients, the Strath PSICAM systematically overestimated data obtained with the HZG PSICAM resulting in an overall best-fit offset of 0.009 m^{-1} . These bulk statistics mask underlying sample to sample variability that is actually rather important for understanding the true nature of the measurement uncertainties. When analysing each sample separately, a strong linear relationship was found for each sample, but the best-fit statistics varied significantly from one sample to the next. Best-fit slopes varied between 0.8 – 1.2 and best-fit offsets were typically $< 0.005 \text{ m}^{-1}$ (average $b(532\text{nm}) = 1.06 \text{ m}^{-1}$), but could reach as high as 0.04 m^{-1} for the samples collected in the Bristol Channel (average $b(532\text{nm}) = 12.85 \text{ m}^{-1}$).

Table 1. Statistical descriptors, slope, offset, R^2 (all obtained from geometric mean linear regression), RMSE, and RMS%E, of absorption spectra measured with PSICAM (CDOM and total), AC-9 (total) and AC-s (total) compared against each other.

	PSICAM vs PSICAM		AC-s vs AC-9	AC-9 vs PSICAM	AC-s vs PSICAM
sample type	total	CDOM	total	total	total
no of samples	63	59	60	56	56
λ [nm]	362-728	362-728	AC-9 wave bands	AC-9 wave bands	400-728
slope	1.02	0.95	0.99	1.23	1.24
offset [m^{-1}]	-0.009	-0.001	-0.031	0.036	0.005
R^2	0.997	0.994	0.989	0.955	0.976
RMSE [m^{-1}]	0.006	0.002	0.028	0.043	0.014
RMS%E [%]	8.0%	12.6%	24.6%	68.6%	30.7%

The same comparison for PSICAM CDOM absorption data also showed a tendency for the HZG PSICAM to underestimate Strath PSICAM absorption coefficients at both ends of the spectrum [Fig. 6(b)] with a geometric mean linear regression slope of 0.95 ($R^2 = 0.994$; Table 1). The distribution of individual sample best-fit slopes was similar to that observed for total non-water absorption data, while the distribution of best-fit offsets was narrower ($< \pm 0.005 \text{ m}^{-1}$).

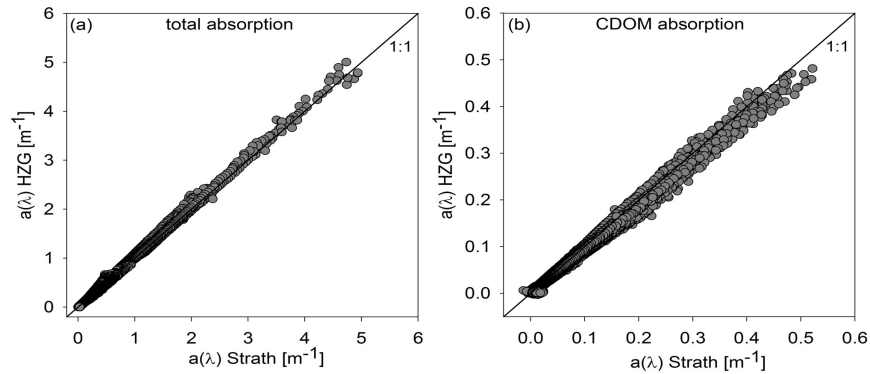


Fig. 6. Comparison of absorption measurements made with the HZG and Strath PSICAM from 362 – 728 nm. (a) total non-water absorption data ($N = 63$), (b) CDOM absorption data ($N = 59$).

As mentioned above, some of this variability is likely to be due to heterogeneity between sub-samples even though care was taken to minimize this during sample preparation. Equally, given the importance that a single sample might have on interpretation of data from a station of particular interest, it is important to have an appreciation of the true range of variability that might be found for an individual sample. Returning to bulk statistics, the challenge is to provide a useful measure of overall accuracy. Root mean square errors (absolute (RMSE) and relative (RMS%E)) were used to describe the overall spread in total non-water absorption data, with $\text{RMSE} = 0.006 \text{ m}^{-1}$ and $\text{RMS}\%E = 8.0\%$. For CDOM absorption determinations, the data spread was smaller than for the total absorption comparison in terms of absolute numbers ($\text{RMSE} = 0.002 \text{ m}^{-1}$) but relatively larger due to the smaller magnitude of absorption signal, resulting in an RMS%E of 13%.

Absolute and relative deviation between the two PSICAMs were found to be wavelength dependent with maximum values at the edges of the spectrum where total (incl. water) sample absorption is high, corresponding to low light intensity levels inside the cavity. Apparent uncertainties increase at the extremes of the spectral range. This can most likely be attributed to artefacts caused by stray light inside the detector, becoming more significant when measured intensity signals are low. Maximum absolute deviation were observed in the blue / UV (high CDOM absorption) and maximum relative deviations were typically found at wavelengths $> 700 \text{ nm}$ where the absorption by water itself increases rapidly [Fig. 7].

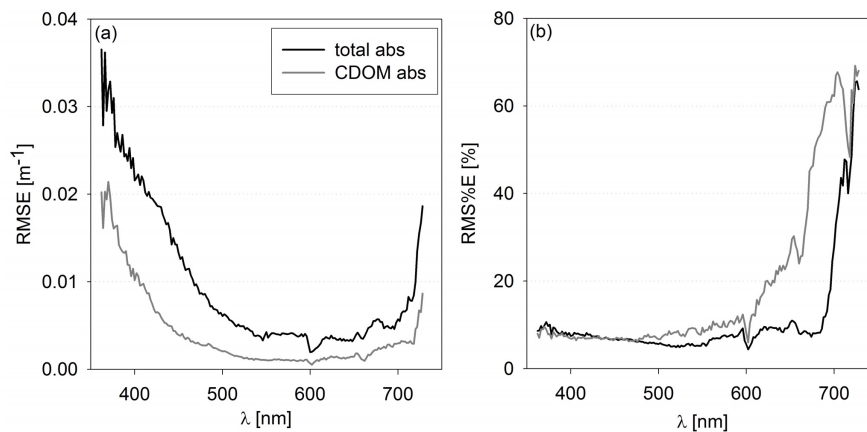


Fig. 7. Wavelength dependency of (a) RMSE and (b) RMS%E derived from comparison of total non-water and CDOM absorption spectra measured with two independent PSICAMs (362 – 728 nm, 2 nm resolution).

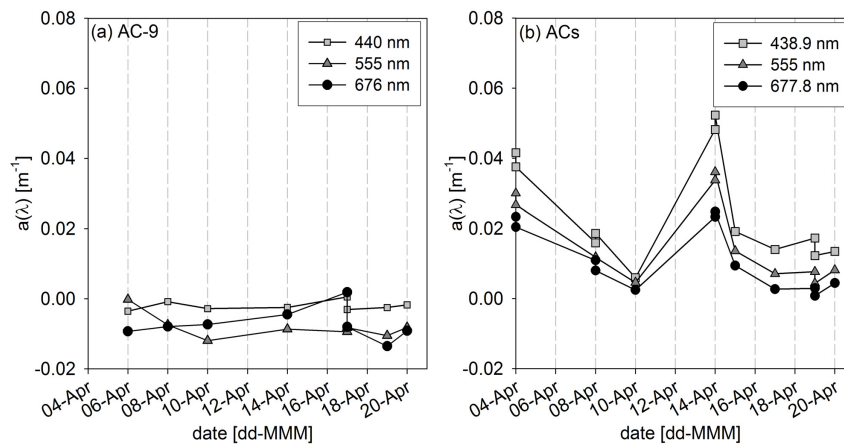


Fig. 8. Time series of on board Milli-Q absorption measurements with (a) an AC-9 and (b) an AC-s at three wavebands (blue, green, red).

3.4 AC-9/s calibration variability

Regular on board measurements of ultrapure water were made for correction of AC-9/s absorption data during subsequent post-processing by subtracting the results as offsets from measured absorption spectra [37]. Figure 8 shows the time series of pure water absorption coefficients at a blue, a green and a red wavelength, obtained throughout the cruise. No consistent trend, indicating drift of the instrument, was observed. However, calibration signal stability on the ship was found to be poor compared to home lab measurements and results showed variation up to 0.015 m^{-1} and 0.046 m^{-1} for the AC-9 and AC-s, respectively [Fig. 8]. This raises major concerns about the data quality of these calibration measurements and about potential bias introduced to absorption data when subtracting these offsets. Since there was no obvious drift in the instruments over time, observed variability in ultrapure water measurements can potentially be attributed to limited data quality associated with practical difficulty of calibrating on the ship's deck, rather than representing actual variability in the instruments' performance. Given the concerns about the quality of on board measurements, two different approaches to process AC-9/s data are available. Data can either be corrected using the average of all calibrations determined over course of the cruise or by applying a more stable calibration performed under laboratory conditions prior to the cruise. For this work, the latter approach was selected and all data presented here was processed using a laboratory calibration.

3.5 AC-9/s precision

At each station a short time series (typically 2.5 – 5 min) of AC-9/s data was collected at the depth at which samples for PSICAM measurements were taken. Raw time series were de-trended by subtracting a 21 point moving average to remove effects of natural variability in the water [Figs. 9 (a) and 9(b)]. Standard deviations of the de-trended time series were calculated to get an estimate for effective instrument precision which is higher than the instrument noise (assessed in purified water calibrations, where standard deviations are $< 0.001 \text{ m}^{-1}$). Figs. 9(c) and 9(d) show histograms of these standard deviations at 440 nm for the AC-9 and AC-s, respectively. Standard deviations for the two instruments were broadly comparable for the two instruments with 58.8% of standard deviations being $\leq 0.01 \text{ m}^{-1}$ for the AC-s ($N = 68$) compared to 48.3% for the AC-9 ($N = 60$). It should be noted, however, that the ranges of these distributions extend to at least 0.03 m^{-1} and in some outlier cases reach as high as 0.1 m^{-1} , even after de-trending to reduce the impact of sample fluctuations during the time series. Once again, it is difficult to completely separate the effects of sample

heterogeneity from intrinsic instrument performance. The precision of both the AC-9 and the AC-s was found to be wavelength dependent with largest absolute uncertainties observed at blue wavelengths and largest relative uncertainties at NIR wavelengths [Fig. 5]. The AC-s showed slightly higher precision compared to its multi-spectral predecessor, which can presumably be attributed to improvements in sensitivity between versions of the instrument and, hence, signal to noise.

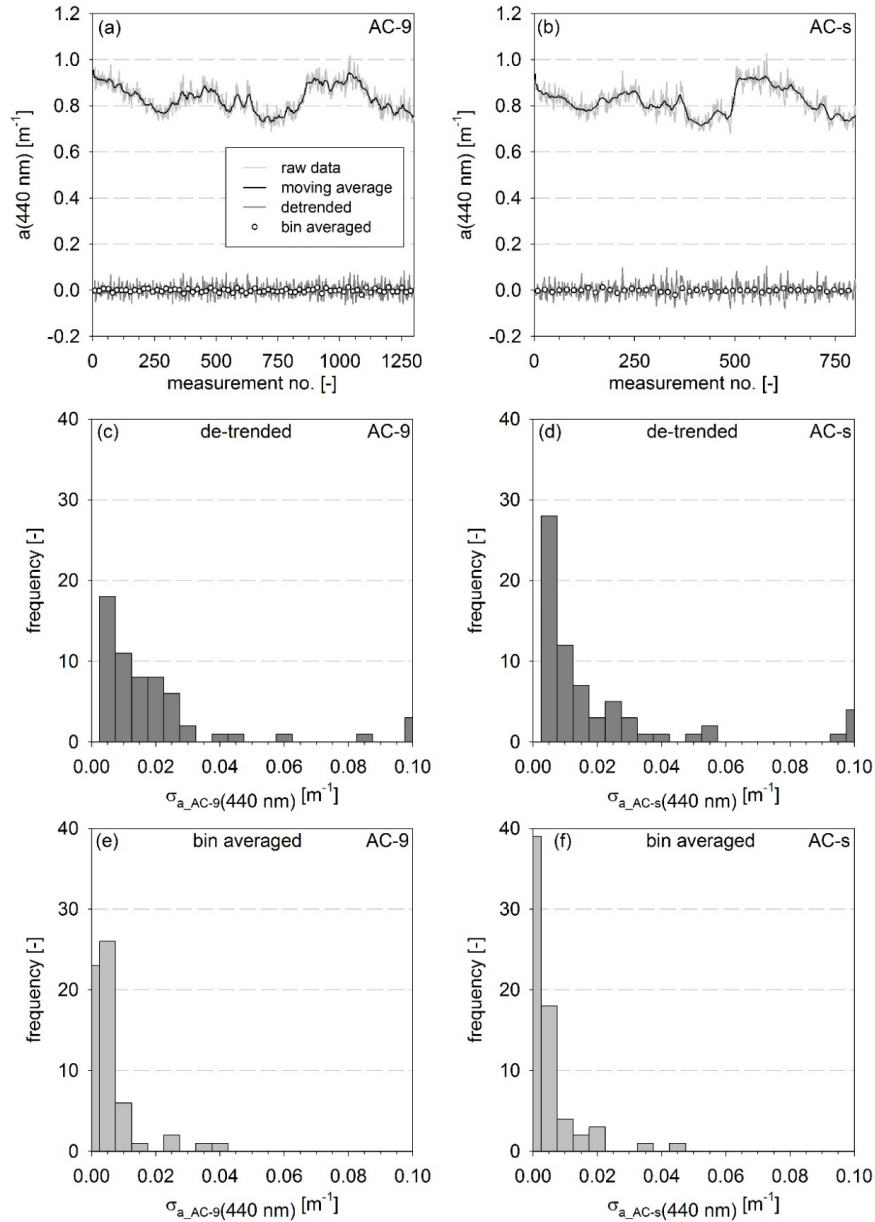


Fig. 9. De-trending time series of (a) AC-9 and (b) AC-s absorption data for standard deviation estimation. Time series were de-trended by subtracting a moving average from time series. (c) & (d) show histograms of standard deviations at 440 nm for AC-9 ($N = 60$) and AC-s ($N = 68$), respectively. (e) & (f) show histograms of standard deviations at 440 nm derived for bin-averaged (18 data points per bin), de-trended time series for AC-9 ($N = 60$) and AC-s ($N = 66$), respectively.

In practice, when AC-9/s instruments are used to measure depth profiles of absorption, data are often averaged to 1 m depth bins. Bin-averaging significantly reduces the variability in absorption data which affects the level of precision of absorption estimates. Figures 9(e) and 9(f) show the effect of bin-averaging on the standard deviation of AC-9/s absorption data at 440 nm. For this analysis, time series were bin-averaged including 18 readings in each bin which is equivalent to the number of readings included in a 1 m depth bin if instruments were lowered at a speed of 0.5 ms^{-1} . Finally, new standard deviations were calculated for each bin-averaged time series resulting in significantly lower estimates, i.e. higher precision, with approx. 84% of AC-9 and AC-s standard deviations at 440 nm being $\leq 0.005 \text{ m}^{-1}$.

3.6 AC-9/s data consistency

Unlike the PSICAM, which is essentially free of scattering errors, the AC-9/s sensors are subject to systematic scattering errors that are not fully addressed by any of the currently available scattering error correction methods. As such, comparison of AC-9 and AC-s data can only provide a measure of data consistency rather than accuracy. The consistency of AC-9/s total non-water absorption coefficients was therefore assessed by comparing AC-s data against AC-9 data at the nine AC-9 wavebands collected at the sampling depths mentioned previously [Fig. 10]. Therefore, raw data were averaged over the same time period of typically several minutes, including natural spatial heterogeneity of samples in the comparison. Data from both instruments was corrected using the semi-empirical correction [16]. Slope and offset derived from geometric mean linear regression ($R^2 = 0.989$) were 0.99 and -0.031 m^{-1} , respectively (Table 1). Data were centred around the 1:1 line with a spread of 0.028 m^{-1} (RMSE) which represents RMS%E of 24.6% for these waters. There is an increasing, apparently systematic divergence between the two instruments at very low signal levels ($< 0.01 \text{ m}^{-1}$) corresponding to a relatively high deviation (RMS%E) at 715 nm which can presumably be attributed to instrument-specific temperature effects and increased sensitivity to limitations in the pure water calibration.

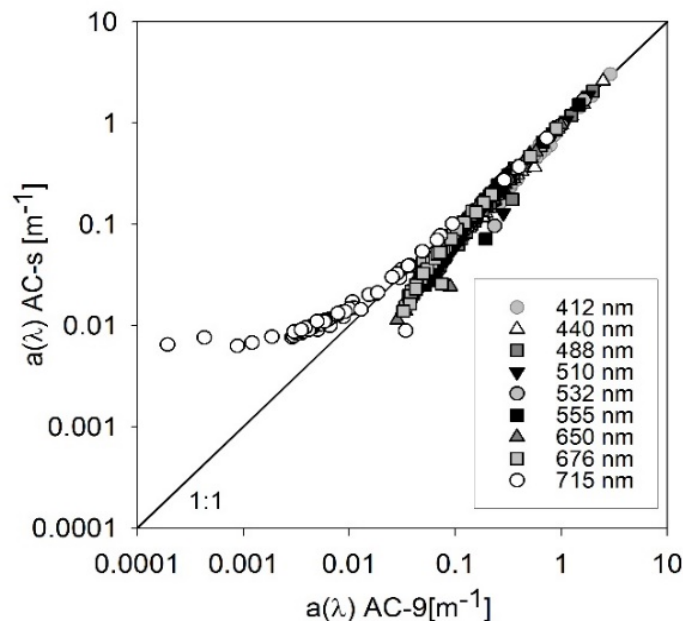


Fig. 10. Comparison of absorption data collected at 57 sampling sites around the UK measured with an AC-9 and AC-s device at 9 different wavebands corrected using the semi empirical correction on a log-log scale.

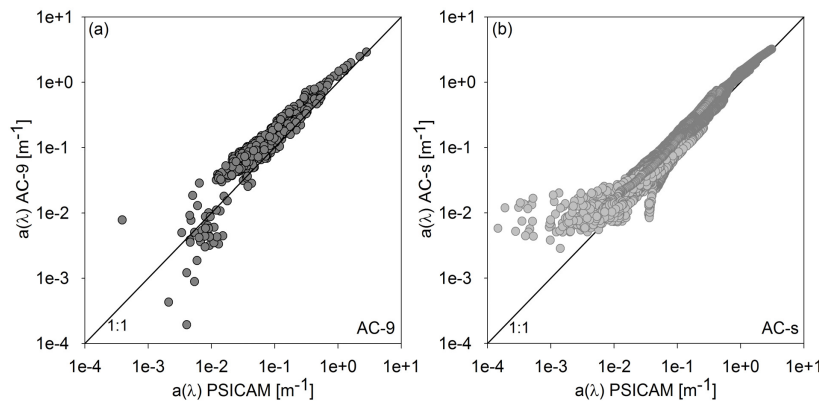


Fig. 11. Comparison of total non-water absorption data collected at 56 sampling sites around the UK measured with (a) an AC-9 (9 wavebands) and (b) and AC-s (400 – 728 nm, at 2 nm resolution) against HZG PSICAM absorption data on log-log-scales.

3.7 Instrument comparison – PSICAM vs. AC-9/s

In a final step, AC-9 and AC-s total non-water absorption data were compared against HZG PSICAM absorption data [Fig. 11]. As expected, agreement between the different techniques was lower than for comparison within the same instrument type. AC-9/s absorption data tended to overestimate PSICAM values, with geometric mean regression slopes of 1.23 and 1.24 and offsets of 0.036 and 0.005 m^{-1} for the AC-9 and AC-s respectively (Table 1). Using all available data, the AC-s showed better agreement with the PSICAM (RMSE = 0.014 m^{-1} , RMS%E = 30.7%) compared to the AC-9 which achieved RMSE of 0.043 m^{-1} and RMS%E of 68.6%. Absolute deviation (RMSE) between AC-9/s and PSICAM absorption data was found to increase with decreasing wavelengths, with largest relative deviations (RMS%E) observed between 550 – 600 nm for the AC-9 and at wavelengths > 700 nm for the AC-s [Fig. 12], where agreement is limited by high pure water absorption and imperfect correction of temperature and salinity effects. Comparison of AC-9/s data with absorption coefficients measured with the Strath PSICAM returned broadly comparable results (data not shown). Given the comparatively low uncertainties observed for the PSICAM, it seems reasonable to assume that the much larger uncertainties observed in Fig. 11 are therefore largely attributable to uncertainties in the AC-9/s data, with corresponding RMSE values being a good order of magnitude estimate of overall accuracy (combining random and systematic uncertainties including bias) for the AC-9/s data.

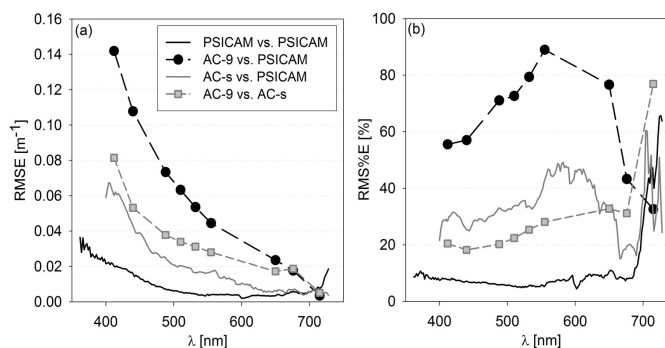


Fig. 12. Wavelength dependency of (a) RMSE and (b) RMS%E derived from comparison of total non-water absorption spectra measured with the Strath PSICAM (362 – 728 nm, 2 nm resolution), AC-9 (9 AC-9 wavebands) and AC-s (400 – 730 nm, 2 nm resolution) against the HZG PSICAM, and of AC-9 absorption vs. AC-s absorption data (at 9 AC-9 wavelengths).

4. Discussion

Both AC-9/s and PSICAM devices have been used for optical studies of marine waters for 10 – 25 years. The reflective tube technology is well established as an industry standard for *in situ* measurements of spectral absorption (NASA Protocols [9]). In light of recent improvements in scattering correction approaches for AC-9/s instruments [16,18], it seems timely to revise and quantify uncertainties associated with AC-9/s absorption measurements beyond scattering errors. The PSICAM technique, on the other hand, is much less widely used because its operation is laborious, despite its potential to produce absorption data that is effectively free from systematic scattering artefacts. To date, no detailed assessment of the magnitude of PSICAM measurement uncertainties has been published. This study uses cross-comparison of two independent PSICAMs and two independent AC-9/s devices to quantify fundamental measurement uncertainties for each absorption measurement technique for the first time.

Precision of absorption determinations with the two different instrument types was quantified using standard deviations at 440 nm. It should be noted, that the precision varies with wavelength and reaches significantly larger values at shorter wavelengths where absorption signals are strongest. However, the analysis presented here focusses on 440 nm to allow comparison with historic studies predominantly using 440 nm as reference wavelength. In the case of the PSICAM, standard deviations were derived using triplicate determinations of the same sample while AC-9/s standard deviations were calculated from de-trended time series. Although the metrics used to assess the precision of PSICAM and AC-9/s devices are not exactly the same, because PSICAM triplicate measurements provide limited information on variability with time, results indicate that AC-9/s absorption measurements have approximately one order of magnitude higher standard deviations and hence equivalently lower precision than absorption determinations with a PSICAM. This broadly reflects differences in effective optical path lengths and a potentially higher sensitivity to sample heterogeneity in AC-9/s instruments. Subsequent bin-averaging of AC-9/s data largely reduces differences in precision to negligible levels. PSICAM averaged standard deviations at 440 nm were found to be 0.002 m^{-1} for CDOM and 0.006 m^{-1} for total non-water absorption determinations. For comparison, the determination of CDOM absorption spectra using a PSICAM provide a similar accuracy and precision compared to measurements with LWCC long-path length systems with path lengths between 50 and 250 cm [34]. The increase in uncertainty for total absorption measurements reflects the increase in natural variability when subsampling from samples with high particle load such as the Bristol Channel, rather than increased scattering effects. AC-9/s precision estimates (average standard deviations at 440 nm) were significantly higher with 0.022 m^{-1} for AC-9 and 0.018 m^{-1} for AC-s measurements despite the fact that the effect of natural variability was reduced by de-trending the raw time series. These estimates reduce to 0.006 m^{-1} (AC-9) and 0.005 m^{-1} (AC-s) when the effect of bin-averaging is taken into account.

Comparing two instruments of the same technique can be used to test the consistency of the method. For total non-water absorption data, the two PSICAMs achieved an agreement within $\pm 0.006 \text{ m}^{-1}$ (RMSE) while the AC-9/s devices showed wider spread with an RMSE of $\pm 0.028 \text{ m}^{-1}$. Apparent systematic relative deviation was largest at wavelengths $> 700 \text{ nm}$ where signal levels are generally low. In PSICAM measurements, there is increased potential for significant systematic artefacts at low measured signals (at both ends of the spectrum), most likely caused by the detector's internal stray light, suggesting that future PSICAM analysis should potentially be restricted to wavelengths between 400–720 nm.

Although it is not possible to determine the true absorption coefficient of a sample, given its relatively high precision and absence of systematic scattering error, PSICAM data has previously been used as a reference for validating other absorption measurements [16,18,31]. Results showed that AC-9/s data typically overestimate PSICAM absorption across the

spectrum and across different water types, with RMSE errors of 0.043 m^{-1} and 0.014 m^{-1} representing average estimates of accuracy statistics for AC-9 and AC-s data respectively. Limited agreement between PSICAM and AC-9/s absorption data potentially reflects real variability as a result of different sampling strategies for each instrument type – both in time (discrete samples do not capture all variability over AC-9/s recording period) and space (offset between AC-9/s intake and Niskin bottle depth). However, the tendency to overestimate absorption can most likely be attributed to residual scattering artefacts in AC-9/s data. This suggests that further work is required to develop a robust scattering correction for a wide range of water types, supporting findings of a recent study showing remaining discrepancies between PSICAM and AC-9 absorption data corrected with the semi-empirical correction [17].

Analysis of measurement uncertainties for each of these instruments raises a philosophical problem with respect to calibration approach. Given that any practical observation is subject to a range of measurement uncertainties, to what extent can any single calibration measurement be trusted as a true representation of the current state of a device? Repetition of calibrations for a particular setup provides information on precision [37], but does not necessarily address accuracy issues e.g. associated with variable water quality, bubbles, etc. As such, is it better to apply most recent calibrations to nearest or subsequent field observations? In the absence of obvious major trends or step changes, measurement uncertainty for each calibration might be sufficiently large that some sort of averaged calibration data would potentially be a better representation of system state. Results presented in this work suggest that apparent variability in calibration determinations recorded over the duration of this field campaign were more likely to originate from uncertainties associated with corresponding measurements rather than represent actual changes in instrument performance. This means that obtaining a robust average estimate from a large number of calibrations performed over a period of general instrument stability might be more beneficial than applying individual calibrations. In the case of the AC-9/s instruments, the stability of instrument calibrations carried out on board the research vessel was sufficiently poor compared to what can be regularly achieved in the home labs that reverting to a pre-cruise calibration potentially offered a more realistic representation of instrument performance.

Measured variability in PSICAM calibrations was found to affect absorption coefficients to varying extents, generally decreasing with wavelength, and corresponding to ~6% of the absorption signal at blue/green wavelengths. The effect of uncertainties in the calibration on absorption data was larger for AC-9/s devices, potentially resulting in very large bias in final absorption coefficients. On board calibration offsets were on average 0.011 m^{-1} (AC-9) and 0.033 m^{-1} (AC-s) compared to a pre-cruise calibration made in much more stable laboratory conditions. Stability of on board AC-9/s calibrations is a general concern. Rapidly changing temperature effects, bubbles and ship movement potentially introduce very large errors in the measurements. At the same time, although such measurements were not found to be particularly reliable for determining new calibration offsets, there is still potential merit in making them on board as they could potentially still reveal the timing of any major shifts in instrument performance that result in sustained deviations from pre-cruise calibrations.

AC-9/s measurement uncertainties discussed here (0.043 m^{-1} (69% RMS%E) and 0.014 m^{-1} (31%), respectively) are larger than typically assumed values ($\pm 0.01 \text{ m}^{-1}$) and hopefully represent more realistic estimates of measurement performance in turbid coastal waters. Accuracy estimates for PSICAM total absorption determinations outperform AC-9/s absorption measurements by approximately an order of magnitude, while precision estimates (after bin-averaging) were found to be broadly comparable. The PSICAM, however, has the disadvantage of relying on discrete samples, potentially failing to capture natural patchiness as well as being susceptible to sample changes due to sample handling and storing. Submersible AC-9/s devices can obviously provide absorption data with much higher spatial / temporal resolution. Until such time as a properly validated *in situ* PSICAM / ICAM sensor

becomes widely available, it is likely that the AC-9/s technology will remain widely used within the community. Understanding the performance characteristics of these instruments is therefore of significant interest both for historic data sets and for new data sets that will be collected in the foreseeable future.

5. Conclusions

Spectral absorption data measured with two PSICAMs and two WET Labs AC-s and AC-9 instruments were compared to assess measurement uncertainties and data consistency. Results showed average overall agreement between PSICAMs within 0.002 m^{-1} (RMSE) for CDOM and 0.006 m^{-1} for total non-water absorption coefficients. The cross-comparison of an AC-9 and an AC-s demonstrated slightly lower consistency with an overall RMS%E of 25% (0.028 m^{-1} RMSE). On average, the two techniques showed a comparable level of precision with at least 84% of standard deviations being within $\pm 0.005 \text{ m}^{-1}$. Precision and accuracy of both techniques varied with wavelengths reflecting a combination of wavelength dependencies in lamp output, wall reflectivity, detector sensitivity, and sample absorption. Increased apparent PSICAM measurement uncertainties at the extremities of spectrum (most likely due to stray light inside the detector) suggested that the quality of absorption data was potentially limited outside the spectral range 400 – 720 nm.

Comparison of the different types of absorption meters (PSICAM vs AC-9/s devices) showed a significantly lower agreement with a maximum overall RMSE of 0.043 m^{-1} for the comparison of AC-9 against PSICAM and a tendency for AC-9/s devices to overestimate PSICAM absorption coefficients. The observed discrepancies can most likely be attributed to insufficient scattering correction of AC-9/s absorption data. The quality of on board calibration measurements of ultrapure water with AC-9/s devices was found to be a major concern and more stable laboratory measurements were used for offset correction of absorption spectra. In comparison, PSICAM calibrations were found to be significantly more stable on board the ship and overall provides approximately an order of magnitude improvement in data accuracy and precision than the AC-9/s devices, albeit with the limitation of being restricted to discrete water samples only.

Funding

Natural Environment Research Council (NERC) (NE/P006302/1); Alfred Wegener Institute Helmholtz Centre for Polar and Marine Research, HE442 cruise on *RV Heincke* (AWI-HE442).

Acknowledgments

The authors would like to thank captain and crew of *RV Heincke* for their support and help during the HE442 research cruise. The cruise with *RV Heincke* was conducted under the grant number AWI-HE442. This work was supported by the NERC Changing Arctic Ocean program (Arctic PRIZE).